see commentary on page 389

Exogenous mesenchymal stem cells localize to the kidney by means of CD44 following acute tubular injury

MB Herrera[1,2], B Bussolati[1,2], S Bruno[1,2], L Morando[1], G Mauriello-Romanazzi[1,2], F Sanavio[3], I Stamenkovic[4], L Biancone[1,2] and G Camussi[1,2]

[1]*Department of Internal Medicine, University of Torino, Torino, Italy;* [2]*Research Centre for Experimental Medicine, Centro Ricerca Medicina Sperimentale (CeRMS), University of Torino, Torino, Italy;* [3]*Division of Hematology, University of Torino, Torino, Italy and* [4]*Division of Experimental Pathology, Institut Universitaire de Pathologie Universite de Lausanne, Lausanne, Switzerland*

Mesenchymal stem cells (MSC) were recently shown to migrate to injured tissues when transplanted systemically. The mechanisms underlying the migration and homing of these cells is, however, unclear. In this study, we examine the role of CD44 and its major ligand, hyaluronic acid, in the trafficking of intravenously injected MSC in the glycerol-induced mouse model of acute renal failure (ARF). *In vitro*, hyaluronic acid promoted a dose-dependent migration of the stem cells that was inhibited by an anti-CD44 blocking monoclonal antibody. *In vivo*, stem cells injected into mice with ARF migrated to the injured kidney where hyaluronic acid expression was increased. Their presence correlated with morphological and functional recovery. Renal localization of the MSC was blocked by pre-incubation with the CD44 blocking antibody or by soluble hyaluronic acid. Stem cells derived from CD44 knockout mice did not localize to the injured kidney and did not accelerate morphological or functional recovery. Reconstitution by transfection of CD44 knockout stem cells with cDNA encoding wild-type CD44, but not a loss of function CD44 unable to bind hyaluronic acid, restored *in vitro* migration and *in vivo* localization of the cells to injured kidneys. We suggest that CD44 and hyaluronic acid interactions recruit exogenous MSC to injured renal tissue and enhance renal regeneration.

Kidney International (2007) **72,** 430–441; doi:10.1038/sj.ki.5002334; published online 16 May 2007

KEYWORDS: stem cells; acute renal failure; hyaluronan; tubular epithelial cells

Correspondence: *G Camussi, Cattedra di Nefrologia, Dipartimento di Medicina Interna, Ospedale Maggiore S. Giovanni Battista, Corso Dogliotti 14, 10126, Torino, Italy. E-mail: giovanni.camussi@unito.it*

Received 11 September 2006; revised 2 April 2007; accepted 10 April 2007; published online 16 May 2007

Mesenchymal stem cells (MSC) are multipotent cells present in bone marrow that can differentiate *in vitro* into adipocytic, chondrocytic, and osteocytic lineages.[1] *In vivo* MSC have been observed not only to regenerate tissues of mesenchymal lineages[2–4] but also to differentiate into neurons[5] and epithelial cells.[6–9]

Acute renal failure (ARF) associated with nephrotoxic and ischemic injury is most often the consequence of acute tubular necrosis.[10] The recovery of renal function following ARF depends on appropriate replacement of necrotic tubular cells with functional tubular epithelium. Key players in kidney regeneration include not only mature proliferating renal cells but also, according to recent reports, stem cells from local pools as well as from the circulation.[11–13] Recent studies in mouse models of ARF have demonstrated that MSC display the ability to localize in damaged kidney promoting both morphological and functional recovery.[8,9] However, to date, mechanisms that underlie MSC homing to injured kidney have not been elucidated.

Tissue injury and inflammation are accompanied by increased stromal production of the glycosaminoglycan hyaluronan (HA), which in addition to other functions, helps to create a low resistance highly hydrated extracellular matrix that may facilitate local cellular trafficking.[14] HA is also abundantly produced in the bone marrow by both stroma and hematopoietic cells[15,16] and it is implicated in the regulation of cell–cell and cell–matrix adhesion as well as in cell proliferation and survival.[17,18] The proteoglycan CD44 is the principal cell surface receptor for HA.[19,20] CD44 is a multifunctional receptor, whose standard isoform is expressed in hematopoietic stem cells[21] and MSC.[22] CD44 has numerous functions, including the regulation of cell proliferation, differentiation, survival, migration into tissues,[20,21] and hematopoietic progenitor trafficking to the bone marrow and spleen.[23–25] Based on these observations, we addressed the role of CD44 receptor and its ligand HA in the recruitment of injected MSC in a mouse model of glycerol-induced ARF.

RESULTS

Soluble HA induced a chemotactic effect on CD44$^+$-MSC

MSC, purified from murine bone marrow, express CD44 (Figure 1a). Therefore, we addressed the possibility that the CD44 ligand HA might have a chemotactic effect on MSC and promote their migration *in vitro*. Consistent with this notion, addition of soluble HA to the lower compartment of a transwell stimulated migration of MSC through polycarbonate filters toward HA (Figure 1b–d). To discriminate between the chemotactic and the chemokinetic effect of HA on MSC migration, studies were performed in the presence of HA on both sides of the Boyden chamber (Table 1). The migratory effect of HA was related to its gradient, suggesting chemotaxis rather than chemokinesis. Preincubation of MSC with a blocking anti-CD44 monoclonal antibody (mAb) (clone KM114) significantly inhibited HA-induced MSC migration (Figure 1b and e).

Expression of HA in the renal cortex after glycerol-induced ARF

Previous work has shown that in normal renal tissue, HA is detectable predominantly in the medulla and hardly if at all in the cortex.[26] We therefore assessed HA expression in injured renal tissue following glycerol-induced ARF. Intramuscular (i.m.) injection of glycerol induces myolysis and hemolysis causing toxic and ischemic tubular injury.[8] Three days after glycerol injection, we observed marked tubular epithelial injury, whereas control mice injected with saline alone displayed no obvious histological change.[8] The lesions observed in mice with ARF included tubular hyaline cast formation, vacuolization, and widespread necrosis of proximal and distal tubular epithelium. Proximal tubules showed cytoplasmic vacuolization, swelling and disorganization of mitochondria, and loss of the brush border. The injured cortical renal tissue contained abundant HA deposits along the tubular basement membrane, whereas no HA was detectable in normal controls (Figure 2a and b).

Characterization of CD44$^{-/-}$- and CD44$^+$-MSC

In this study, we investigated whether CD44/HA interaction is instrumental in the localization of exogenous MSC in the injured kidneys. For this purpose, we obtained and purified

Table 1 | Gradient-dependent analysis of HA-induced migration

	Upper chamber		
Lower chamber	Vehicle	20 μg/ml HA	200 μg/ml HA
Vehicle	13.3 $\pm$ 1.53	22.7 $\pm$ 11.59	12.3 $\pm$ 2.52
20 μg/ml HA	42.3 $\pm$ 1.78	24 $\pm$ 4.36	10.7 $\pm$ 2.08
200 μg/ml HA	44.3 $\pm$ 3.79	21.3 $\pm$ 1.53	13.7 $\pm$ 2.52

Migration of MSC was performed in Boyden chambers by adding HA in the upper and/or lower compartments to establish positive, negative, absent gradient across the filter barrier.

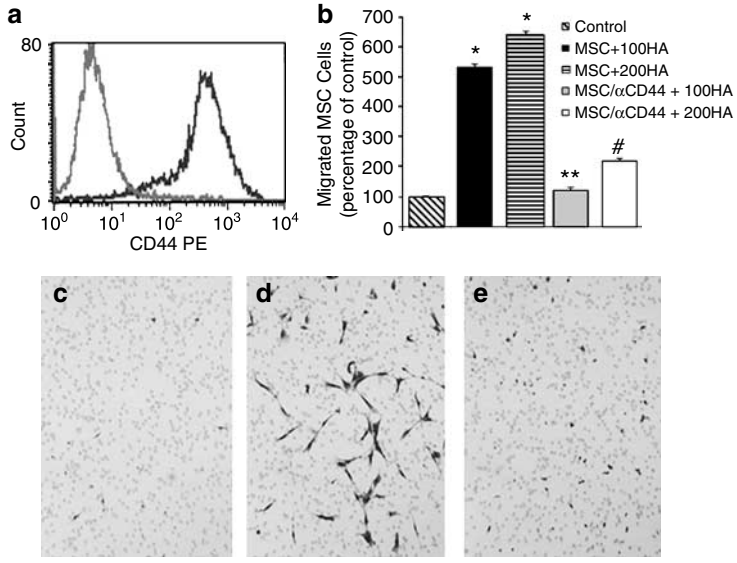

Figure 1 | HA–CD44 interaction induced *in vitro* migration of MSC. (**a**) FACS analysis of CD44$^+$-MSC showing expression of CD44 in 100% of cells (10 different MSC preparations were examined with similar results). (**b–e**) *In vitro* migration assay of MSC preincubated or not with 5 μg/ml blocking CD44 mAb (MSC/αCD44) and stimulated with HA. MSC were seeded in the upper side of the transwell, and HA (100 and 200 μg/ml indicated as 100HA and 200HA) in the lower compartment, as described in Materials and methods. Migration was evaluated after 18 h incubation at 37°C by counting the cells that passed through the 8-μm membrane pores. The filters were fixed and stained with Diff-Quick. (**b**) The percentage of increased MSC migration after incubation with HA in respect to control challenged with vehicle alone. Values are expressed as % with respect to control and are the mean $\pm$ s.d. of three independent experiments run in triplicate. ANOVA with Newmann–Keuls' multicomparison test was performed: *$P < 0.05$ MSC + 100HA and MSC + 200HA vs vehicle; **$P < 0.05$ MSC/αCD44 + 100HA and vs MSC + 100HA; $^{\#}P < 0.05$ MSC/αCD44 + 200HA vs MSC + 200HA. (**c–e**) Representative micrographs of MSC migration. Only few MSC migrated to the lower side of the membrane when challenged with vehicle alone (**c**); several MSC migrated to the lower side of the membrane when challenged with 100 μg/ml HA (**d**) but not when preincubated with 5 μg/ml blocking CD44 mAb and challenged with 100 μg/ml HA (**e**). (Original magnification $\times$ 200).

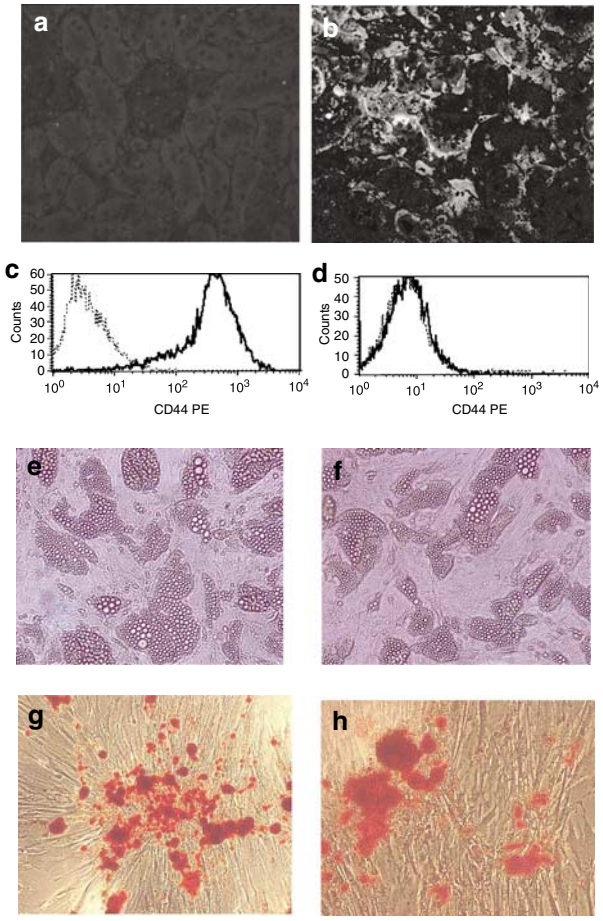

Figure 2 | Effect of glycerol-induced tubular injury on HA expression by renal cortex and characterization of bone marrow-derived CD44$^+$-MSC and CD44$^{-/-}$-MSC. (**a**) Representative micrographs of a cryostat section of renal cortex from a control mouse killed 3 days after i.m. injection of vehicle alone showing absence of immunofluorescent staining for HA expression evaluated with a soluble CD44H-human Ig fusion protein (0.5 μg/ml) (original magnification $\times$ 250). (**b**) Representative micrographs of a cryostat section of renal cortex of a mouse killed 3 days after i.m. injection of glycerol showing a positive immunofluorescence staining along tubular basement membrane and interstitium for HA expression (original magnification $\times$ 250). Ten mice were examined per group with similar results. (**c**) Representative flow cytometric analysis of CD44$^+$-MSC showing the expression of CD44. (**d**) Representative flow cytometric analysis of CD44$^{-/-}$-MSC showing that MSC obtained from CD44$^{-/-}$ mice were negative for CD44. The dark line is the test antibody, the dotted line the isotypic control. (**e**–**f**) Representative micrographs of adipogenic differentiation of CD44$^+$- and CD44$^{-/-}$-MSC detected by the presence of fat droplets. (**g**–**h**) Representative micrographs of osteogenic differentiation detected by positive staining for calcium deposits using Alizarin Red. (Original magnification **c**–**f**: $\times$ 250). Ten different cells preparations were tested with similar results.

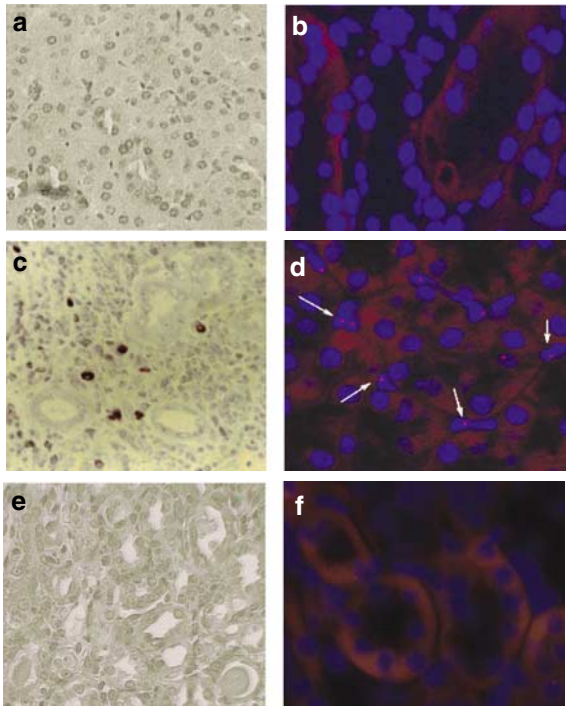

Figure 3 | Role of CD44 in renal homing of MSC in mice with glycerol-induced ARF. MSC were detected by immunoperoxidase staining of CFSE or by FISH analysis of Y chromosome 24 h after their injection. (**a**–**b**) Representative micrographs showing the absence of MSC in renal sections of a mouse without ARF injected with CD44$^+$-MSC. (**c**–**d**) Representative micrographs showing localization of MSC in renal sections of a mouse with ARF injected with CD44$^+$-MSC. (**e**–**f**) Representative micrographs showing the absence of MSC in renal sections of a mouse with ARF injected with CD44$^{-/-}$-MSC. Original magnification: immunoperoxidase (**a**, **c** and **e**) $\times$ 250; FISH analysis (**b**, **d** and **f**; arrows indicate the positive staining for chromosome Y) $\times$ 600.

MSC from the bone marrow of CD44$^{-/-}$ and CD44$^+$ mice. CD44$^{-/-}$-MSC (at the fourth passage) expressed the common mesenchymal markers CD105, CD29, CD73 (not shown) similarly to CD44$^+$-MSC, but not CD44 (Figure 2c and d), as assessed by cytofluorimetric analysis. In addition, MSC from CD44$^{-/-}$ and CD44$^+$ mice expressed the stem cell marker Thy1 (CD90), but not the leukocyte marker CD45 and CD14 or KDR, a marker of circulating endothelial progenitor cells (data not shown). Absence of CD34 expression indicated that no contaminating hematopoietic stem cells were present. No functional differences between CD44$^{-/-}$ and CD44$^+$-MSC were observed in terms of their differentiation potential toward adipocytic (Figure 2e and f) and osteogenic lineages (Figure 2g and h). However, the growth rate of CD44$^{-/-}$ cells was approximately half of that of wild-type CD44$^+$-MSC (data not shown), consistently with the reported role of CD44 in cell proliferation.[27]

Role of CD44–HA interaction in renal recruitment of MSC

In the glycerol-induced model of acute renal injury, CD44$^+$ or CD44$^{-/-}$-MSC were injected 3 days after glycerol administration. Twenty-four hours after injection, CD44$^+$-MSC were detected within the renal cortex of mice with ARF by immunoperoxidase staining of carboxy-fluorescein diacetate, succinimidyl ester (CFSE)-labelled MSC, by fluorescence *in situ* hybridization (FISH) detection of Y chromosome and by iron detection in iron-dextran-labelled MSC (Figures 3–5).

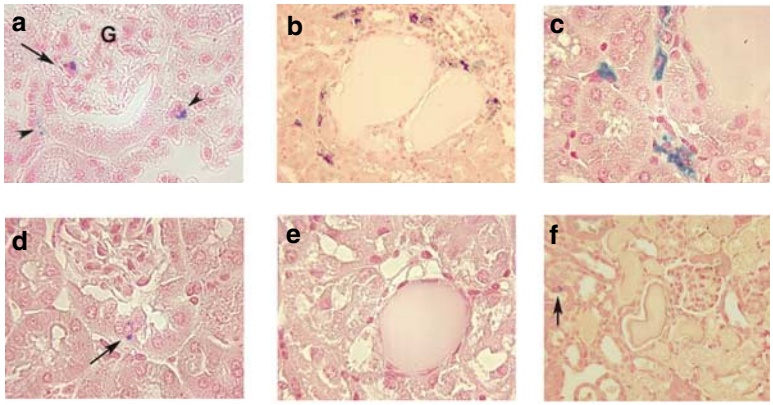

Figure 4 | MSC detection by light microscopy in mice with glycerol-induced ARF by iron-dextran labelling 24 h after their injection. (**a**–**d**) Representative micrographs showing localization of $CD44^+$-MSC in renal sections of a mouse with ARF. (**a**) The presence of iron-dextran-labelled $CD44^+$-MSC in a glomerulus (**g**; arrow) and in peritubular capillaries (arrowheads). (**b** and **c**) The concentration of iron-dextran-labelled $CD44^+$-MSC around severely damaged tubules containing protein casts. (**c**) Is a particular of panel (**b**) clearly showing the interstitial localization of labelled MSC. (**e**) Presence of an isolated iron-dextran-labelled $CD44^+$-MSC (arrow) within a proximal tubule. (**e** and **f**) Absence or presence of a rare iron-dextran-labelled $CD44^{-/-}$-MSC (arrow) in renal sections of a mouse with ARF. The sections were stained with Prussian blue. Original magnification (**a**, **d** and **e**) $\times$400; (**c**) $\times$600; (**b**); and (**f**) $\times$250.

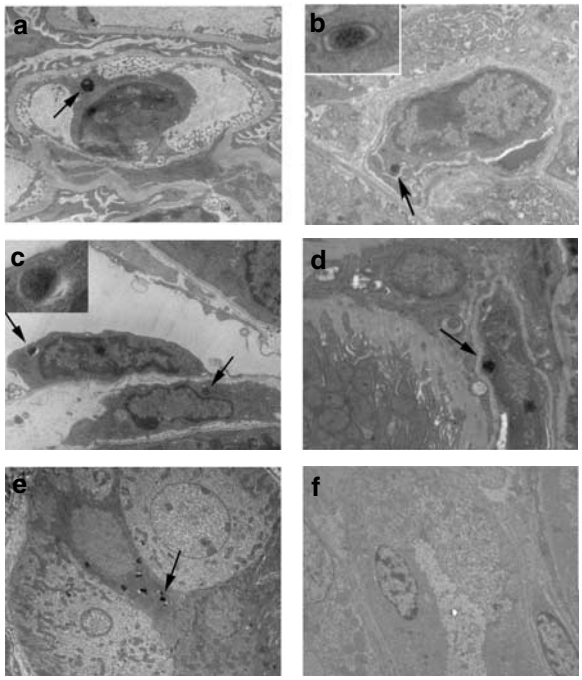

Figure 5 | MSC detection by electron microscopy in mice with glycerol-induced ARF by iron-dextran labelling 24 h after their injection. (**a**–**e**) Representative micrographs showing localization of iron-dextran-labelled $CD44^+$-MSC in renal ultrathin sections of a mouse with ARF observed by transmission electron microscopy. (**a**) shows the presence of a MSC within the lumen of a glomerular capillary. The arrow indicates the iron-dextran inclusion. (**b**–**d**) show the presence of iron-dextran-labelled $CD44^+$-MSC in the peritubular capillaries (**b** and **c**) and in the interstitium. In (**c**), a cell adherent to the endothelial layer and a cell infiltrated in the subendothelial space are shown. Arrows indicate the iron inclusions. The insets in (**b** and **c**) show high magnification of the iron-dextran inclusions. (**e**) A cell containing iron-dextran inclusions (arrow) infiltrating a proximal tubule. (**f**) The absence of iron-dextran-labelled $CD44^{-/-}$-MSC in a renal section of a mouse with ARF. Original magnification $\times$6000; insets $\times$25 000.

The labelled cells were observed within peritubular capillaries and the interstitial space (Figures 3c and d, 4b and c and 5b–d). Few cells were also detected in the glomeruli (Figures 4a and 5a). Very few labelled cells were observed within tubular epithelium (Figure 4d and 5e). No cells were detected in control mice without ARF injected with $CD44^+$-MSC (Figure 3a and b). In mice with ARF injected with $CD44^{-/-}$-MSC, only rare cells could be detected within the renal cortex (Figure 3e and f, 4e and f, and 5f). The typical iron inclusions observed by electron microscopy (Figure 5b and c, insets) were absent in control ARF mice, suggesting that they were not due to uptake of iron due to hemolysis. Minimal localization of MSC was observed in the renal medulla (not shown), despite the constitutive presence of HA, suggesting that release of HA fragments by inflammation and of other factors produced by the injured tissue are required for MSC recruitment.

To further confirm the role of HA binding by CD44 in the early localization of MSC in the injured kidney, we performed reconstitution experiments by transfection of $CD44^{-/-}$-MSC with cDNAs encoding either functional wild-type CD44 or the CD44R41A mutant, that lacks the ability to bind the HA (CD44HMut)[28] (Figure 6). As expected, fluorescein isothiocyanate (FITC)-labelled HA bound $CD44^+$-MSC but not $CD44^{-/-}$-MSC (Figure 6a and b). Transfection of $CD44^{-/-}$-MSC with full-length CD44H (CD44H MSC) restored their ability to bind HA, whereas expression of CD44Hmut (CD44HMut MSC) failed to do so (Figure 6f and g), despite CD44 antigen expression, as assessed by immunofluorescence (Figure 6c–e). Migration assay showed that transfection with full-length CD44H, but not with CD44Hmut, restored chemotaxis to HA (Figure 6h), suggesting a functional reconstitution of CD44.

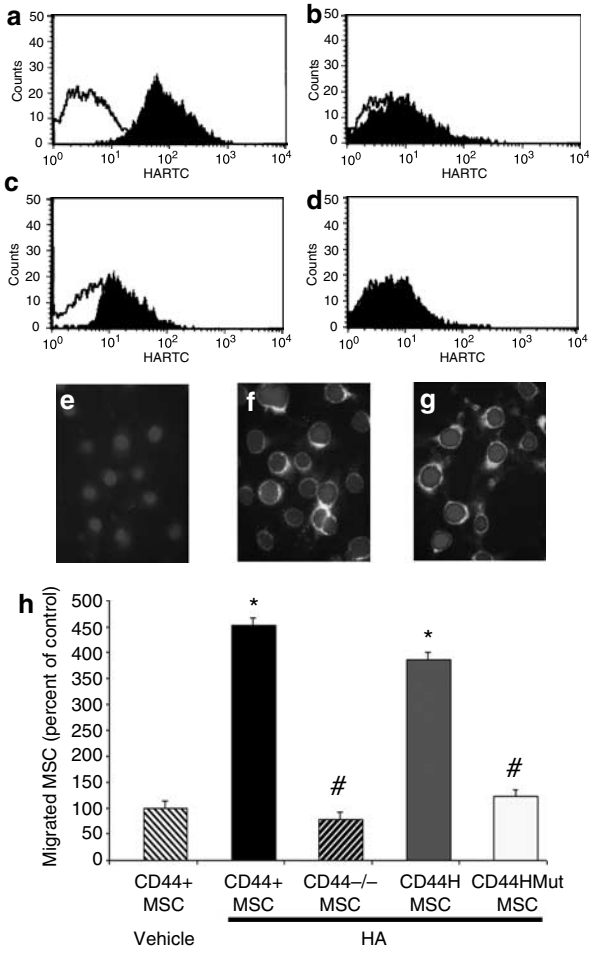

Figure 6 | Reconstitution of CD44$^{-/-}$-MSC with functional or non-functional CD44. CD44^{+}-MSC, CD44$^{-/-}$-MSC, and CD44$^{-/-}$-MSC transfected with a full-length CD44 cDNA (CD44H) or with a mutant form of CD44 cDNA (CD44HMut) transfectant were generated. (**a**–**d**) Representative flow cytometric analysis of FITC-labelled HA-binding on CD44^{+}-MSC, CD44$^{-/-}$-MSC and trasfectants. (**a** and **b**) The FITC-labelled HA-binding to (**a**) CD44^{+}-MSC but not (**b**) CD44$^{-/-}$-MSC. (**c** and **d**) The FITC-labelled HA-binding to (**c**) CD44H but not to (**d**) CD44Hmut. The gray area is FITC-labelled HA and the dark line is FITC-labelled bovine serum albumin, used as control. Three different cells preparations were examined with similar results. (**e**–**g**) Representative micrographs of immunofluorescence analysis with anti-human CD44 (clone A3D8) mAb of CD44$^{-/-}$-MSC transient transfected (**e**) with an empty vector, (**f**) with a full-length CD44 cDNA or (**g**) with a mutant form of CD44 cDNA. (Original magnification: $\times$ 200). (**h**) *In vitro* migration assay of CD44^{+}-MSC, CD44$^{-/-}$-MSC, and trasfectants. MSC were seeded in the upper side of the transwell, and HA (100 μg/ml) in the lower compartment, as described in Materials and methods. Migration was evaluated after 18 h incubation at 37°C by counting the cells that passed through the 8-μm membrane pores. The filters were fixed and stained with Diff-Quick. Data show the percentage of increased MSC migration after incubation with HA in respect to control challenged with vehicle alone. Values are expressed as % with respect to control and are the mean $\pm$ s.d. of three independent experiments run in triplicate. ANOVA with Dunnett's multicomparison test was performed *$P < 0.05$ MSC stimulated with HA vs MSC stimulated with vehicle.

As shown in Figure 7, the percentage of labelled MSC detected in the renal cortex 24 h after injection was significantly different in mice injected with CD44$^{-/-}$-MSC in respect to CD44^{+}-MSC. Moreover, CD44H MSC but not CD44HMut MSC significantly localized in the injured kidneys (Figure 7a), suggesting that the binding of CD44 to HA is critical for MSC homing. The role of CD44 in MSC localization was further confirmed by the inhibition of MSC localization when pre-incubated with either an anti-CD44 blocking mAb or soluble HA (Figure 7b).

Role of CD44^{+}-MSC in the recovery of renal injury

Eight days after damage (5 days after MSC injection), an extensive recovery with regeneration of tubular epithelial cells and of the cell brush border was observed in mice injected with CD44^{+}-MSC (Figure 8a). In contrast, mice injected with CD44$^{-/-}$-MSC displayed persistence of diffuse necrotic proximal and distal tubule injury (Figure 8c). At day 8, only scattered CD44^{+}-MSC were present within the renal interstitium, whereas the CFSE-labelled and chromosome Y-labelled cells were mainly detectable within the proximal tubules (Figure 8b). The number of CFSE-positive MSC counted in immunoperoxidase-stained sections was $2.2 \pm 0.4\%$ in respect to the total number of counted nuclei. No CD44$^{-/-}$-MSC were detectable at day 8 (Figure 8d). The morphologic recovery induced by administration of CD44^{+}-MSC was accompanied by recovery of the renal function. Blood urea nitrogen (BUN) levels that peaked at day 3 following ARF induction were significantly reduced at day 8 in the animals that had received CD44^{+}-MSC (Figure 9a). In contrast, CD44$^{-/-}$-MSC injection did not significantly affect the BUN levels, that persisted elevated at day 8 as in the untreated mice (Figure 9a). To evaluate whether the expression of CD44 affects the severity and the recovery of glycerol-induced ARF, we compared wild-type and CD44$^{-/-}$ mice. As shown by BUN levels, the severity of ARF was significantly lower in CD44$^{-/-}$. However, the increased BUN persisted at day 8, suggesting that the absence of recruitment of inflammatory cells in CD44$^{-/-}$ mice protected mice from glycerol-induced ARF (Figure 9b), as previously described for ischemic injury.[29] However, in these animals, a significant recovery from day 3 to day 8 was not observed as also inferred by histological analysis (not shown).

To evaluate whether MSC may differentiate into epithelial cells, the presence of CFSE-labelled CD44^{+}-MSC expressing epithelial markers was detected by fluorescence-activated cell sorter (FACS) analysis in cells obtained from disaggregated tubular component of renal tissue of ARF mice at day 8. As shown in Figure 10a, the population of fluorescent CFSE-positive cells observed in CD44^{+}MSC-treated animals amounted to $2.3 \pm 0.2\%$ of five experiments. No auto-fluorescent cell population was detected in control mice without or with ARF that had not been injected with MSC (Figure 10a). Co-staining with CFSE and the epithelial tubular markers, lens culinaris agglutinin, megalin, and cytokeratin, showed that at least a fraction (respectively,

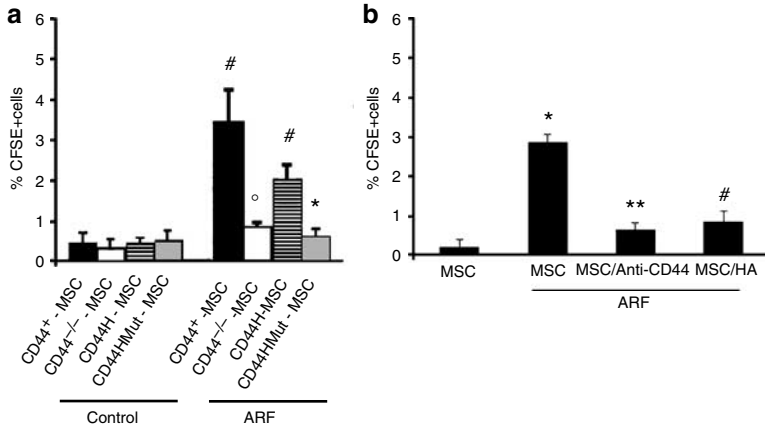

Figure 7 | Localization of CD44$^+$-MSC but not CD44$^{-/-}$-MSC in kidneys of mice with ARF 24 h after injection. CD44$^+$-MSC, CD44$^{-/-}$-MSC, and CD44$^{-/-}$-MSC transfected with a full-length CD44 cDNA (CD44H) or with a mutant form of CD44 cDNA (CD44HMut) transfectant were generated and injected in ARF mice. (**a**) count of CFSE-labelled MSC within renal tissue of control mice without ARF or of mice with glycerol-induced ARF that were injected with CD44$^+$-MSC, CD44$^{-/-}$-MSC, or CD44H MSC or CD44HMut MSC evaluated 24 h after injection. The number of CFSE-positive MSC was counted in 10 non-sequential sections for each experiment at $\times$200 magnification and expressed as % in respect to the total number of counted nuclei. Data are expressed as mean count $\pm$ s.d. of CFSE-labelled MSC detected by immunohistochemical staining of 12 different mice. ANOVA with Newmann–Keuls' multicomparison test was performed: $^{\#}P<0.05$ ARF + CD44H MSC vs CD44H MSC without ARF and ARF + CD44$^+$-MSC vs CD44$^+$-MSC without ARF; $^{\circ}P<0.05$ ARF + CD44$^{-/-}$-MSC vs ARF + CD44$^+$-MSC; $^{*}P<0.05$ ARF + CD44HMut MSC vs ARF + CD44H MSC. (**b**) Reduction of the renal localization of CD44$^+$-MSC 24 h after injection when cells were preincubated for 30 min with 5 μg/ml blocking CD44 mAb (MSC/αCD44) or with 200 μg/ml soluble HA (MSC/HA). Data are expressed as mean count $\pm$ s.d. of CFSE-labelled MSC detected by immunohistochemical staining in 10 fields per kidney of three different mice. ANOVA with Newmann–Keuls' multicomparison test was performed: $^{*}P<0.05$ ARF + MSC vs MSC; $^{**}P<0.05$ ARF + MSC/αCD44 vs ARF + MSC; $^{\#}P<0.05$ ARF + MSC/HA vs ARF + MSC.

26.2% $\pm$ 9.65, 21.0% $\pm$ 6.08, 64.2% $\pm$ 17.28 of five experiments) of CFSE-positive cells recovered from the kidney expressed epithelial differentiation markers (Figure 10b). Before injection, MSC did not express any of these epithelial markers (Figure 10b). When CFSE-labelled CD44$^{-/-}$-MSC were injected in ARF mice, only very few fluorescent cells were detected (Figure 10a). To evaluate whether MSC fused with epithelial cells in the kidney, we studied the DNA content of the CFSE-positive population by FACS analysis. As shown in Figure 10c, the CFSE-positive cells showed a ploidy of 2N, rather than 4N, indicating that a significant fusion did not occur.

DISCUSSION

Migration towards sites of tissue injury is the first step of stem cell-mediated tissue regeneration. Homing of MSC into injured tissues relies upon their ability to migrate to and interact with the local microenvironment in a manner that secures their anchorage at sites where their effector functions are required.

We have shown here that expression of cell surface CD44 is involved in the localization of exogenous MSC to injured renal tissue based on the observations that loss of CD44 expression by MSC or expression of a CD44 loss-of-function mutant results in ineffective MSC localization to injured tissue and inhibition of renal repair.

Several studies suggest that MSC may contribute to the recovery of acute tubular injury.[8,9,30] It remains however uncertain whether bone marrow-derived stem cells may be a source of regenerating tubular cells or rather contribute to tubular recovery by a mechanism of protection.[31] Independently from the mechanism involved in renal repair, the local recruitment of MSC is a condition necessary for their beneficial effect.[31] Currently, little is known about the molecular mechanisms that underlie MSC recruitment. Recent studies suggest that triggering of the chemokine receptor CXCR4 by its ligand stromal derived factor may play an important role in the migration of transplanted MSC to sites of injury in the brain,[32] even though CXCR4 appears to be expressed at a low level on the surface of MSC.[33] Although it is likely that several mechanisms, including chemokine–chemokine receptor interactions and possibly several adhesion receptor-ligand pairs, participate in MSC homing, CD44–HA interaction may provide a dominant force in guiding MSC to appropriate repair/regeneration sites. The importance of CD44-mediated cell interaction with HA for the regulation of cell migration has been shown in several biological processes, including inflammation and tumor metastasis.[34–39] Recently, it has been shown that CD44–HA interaction is involved in MSC migratory capacity.[37] In line with this study, we found that HA-mediated *in vitro* migration of MSC is prevented by preincubation with an anti-CD44 blocking Ab or soluble HA. HA, the principal CD44 ligand,[19] has been suggested to drive recruitment of hematopoietic stem and progenitor cells to the bone marrow.[23,24] However, the potential role of CD44 in MSC homing to injured tissue had so far not been addressed. HA is barely detectable in many normal tissues in the resting state

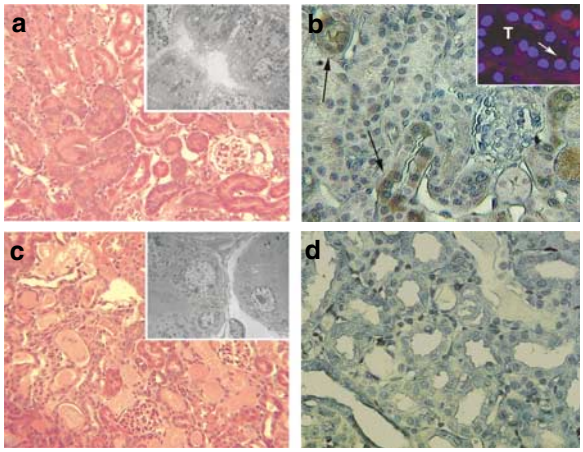

Figure 8 | Role of CD44$^+$-MSC in morphological renal recovery in mice 8 days after ARF induction. Micrographs are representative of glycerol-induced acute tubular injury after CD44$^+$-MSC and CD44$^{-/-}$-MSC injection. (**a** and **b**) Morphological recovery of renal damage and CD44$^+$-MSC renal localization in mice with ARF injected i.v. with 1×10^6 CD44$^+$-MSC 3 days after receiving the i.m. injection of glycerol and killed 5 days after the MSC administration (day 8). Representative micrographs of a light microscopy section stained with haematoxylin eosin (**a**: original magnification $\times 250$) and of electron microscopy (inset: original magnification $\times 4000$) showing the recovery of tubular injury. (**b**) Detection of CFSE-labelled CD44$^+$-MSC by immunohistochemistry (original magnification $\times 250$) and by detection of Y chromosome by FISH (inset: original magnification $\times 600$) showing the presence of CFSE-positive and Y chromosome-positive cells within some tubules (arrows; T = tubule). (**c** and **d**) morphological alterations and CD44$^{-/-}$-MSC renal localization in mice with ARF injected i.v. with 1×10^6 CD44$^{-/-}$-MSC 3 days after receiving the i.m. injection of glycerol and killed 5 days after the MSC administration (day 8). Representative micrographs of a light microscopy section stained with haematoxylin eosin (**c**: original magnification $\times 250$) and of electron microscopy (inset: original magnification $\times 4000$) showing the persistence of severe tubular injury. (**d**) Absence of localization of CFSE-labelled CD44$^{-/-}$-MSC by immunohistochemistry (**i**: original magnification $\times 250$). Twelve mice were examined per group with similar results.

and, whereas it is abundant in the renal medulla, it is virtually absent from the cortex of normal kidney.[26] However, tissue remodelling associated with development, inflammation, repair, and cancer invasion is accompanied by robust induction of stromal HA production and deposition. Accordingly, 3 days after induction of ARF by glycerol injection, HA deposition was readily detectable in the interstitium and along the tubular basement membrane in renal cortex. Similar observations have been made following induction of ischemia-reperfusion injury.[40]

The migratory effect of soluble HA on MSC that we observed in this study was related to its gradient, suggesting a chemotactic mechanism. During injury, it is conceivable that protease-induced matrix degradation may release soluble HA fragments that may contribute to the recruitment of MSC.

In this study, we demonstrate that localization of exogenous MSC to injured renal tissue is dependent on the CD44–HA interaction. The CD44$^+$-MSC were detectable within peritubular vessels and the interstitium 24 h after injection, consistent with other studies that demonstrated the early recruitment of MSC to the kidney.[41] In contrast, MSC derived from CD44$^{-/-}$ mice failed to localize to the injured tissue. Disruption of CD44/HA interaction by pre-incubation with anti-CD44 mAb or soluble HA confirmed the relevance of a functional CD44 for MSC recruitment. Indeed, transfection of CD44$^{-/-}$ MSC with functional CD44, but not with a CD44 loss-of-function mutant, restored the recruitment of MSC. This result, together with experiments of CD44 blockade, indicates that CD44 has a critical role in the localization of exogenous MSC in the kidney. However, we cannot exclude that extrarenal events may contribute to the reduced renal accumulation of CD44$^{-/-}$ cells.

The recruitment of MSC within the injured kidney accelerated the functional and morphological recovery. Using whole-bone marrow transplantation in the mouse, Poulsom *et al.*[42] demonstrated that bone marrow-derived cells could contribute to regeneration of the renal tubular epithelium. It is debated whether bone-marrow-derived stem cells contribute to renal recovery by fusion or transdifferentiation into tubular epithelial cells. Duffield *et al.*[43] showed that bone marrow does contain cells capable of protecting the kidney from ischemic injury, but these cells were not directly incorporated into the repaired tubules. Lin *et al.*[44] found that only a minority of bone marrow-derived cells were incorporated into the injured tubules as epithelial cells. Broekema *et al.*[45] demonstrated that the tubular engraftment of bone marrow-derived cells depends on the severity of renal damage after ischemia/reperfusion injury and that once engrafted these cells acquire an epithelial phenotype. The results of this study showed that after 24 h, the injected MSC were mainly detectable within the peritubular capillaries and interstitium, whereas after 8 days MSC were found mainly within tubules. The experiments with CFSE-labelled MSC followed by their recovery from the tissue indicate that about 2–2.5% of the cells recovered from the renal cortex at day 8 derived from the injected MSC. Fang *et al.*[46] found some evidence for cell fusion between resident renal tubular cells and bone marrow-derived cells, but this was infrequent and the significance and consequences of cell fusion in the kidney are still unclear. In this study, we found that CFSE-positive cells showed a ploidy of 2N rather than 4N, suggesting that a significant fusion did not occur. Moreover, the number of MSC detectable in the renal injured tissue was not increased at 8 days in respect to the 24 h, suggesting a minor role of MSC in the repopulation of tubules. These data are consistent with a previously reported prominent role of proliferation of resident cell in the repopulation of tubules.[43–46] Owing to their low number, the repopulation of tubules cannot be ascribed to the transdifferentiation of the injected MSC but rather to a beneficial paracrine effect. MSC may favor de-differentiation and proliferation of the surviving tubular cells or stimulation of resident stem cells.[11,31] Moreover, MSC possess an anti-inflammatory[31] and immunosuppressive potential[47,48] that may be involved in the protection of tissue injury. On the other hand, the ability of bone-marrow-derived stem cells to transdifferentiate and contribute to

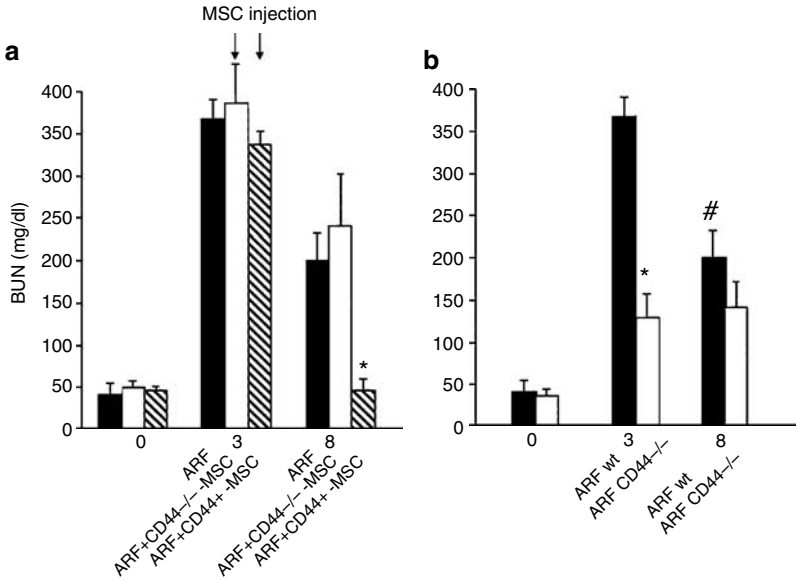

Figure 9 | Evaluation of renal function in wild-type mice injected with CD44^{+} or CD44$^{-/-}$-MSC, and in CD44$^{-/-}$ mice 3 and 8 days after glycerol-induced ARF. (**a**) Evaluation of BUN in CD44^{+}-MSC, CD44$^{-/-}$-MSC, and MSC untreated mice before, 3 and 8 days after glycerol injection. MSC (arrows) were injected at day 3. Injection of CD44^{+}-MSC but not of CD44$^{-/-}$-MSC enhanced the recovery of the renal function. Each group consisted of 12 mice. Data are expressed as mean ± s.d. and ANOVA with Newmann–Keuls' multicomparison test was performed: *$P<0.05$ ARF + CD44^{+}-MSC vs ARF + CD44$^{-/-}$-MSC. (**b**) Comparison of the BUN levels in wild-type (wt) or CD44$^{-/-}$ mice before, 3 and 8 days after glycerol injection. The increase of BUN in CD44$^{-/-}$ mice was significantly lower then in wild-type mice at day 3. At day 8, the spontaneous recovery was significant in wild-type mice but not in CD44$^{-/-}$ mice. Each group consisted of 12 mice. Data are expressed as mean ± s.d. and ANOVA with Newmann–Keuls' multicomparison test was performed: *$P<0.05$ ARF CD44$^{-/-}$ mice vs ARF wt mice; $^{\#}P<0.05$ day 8 vs day 3.

podocyte regeneration has been recently shown in a murine model of Alport syndrome.[49,50]

Tissue injury of a broad range of etiologies is associated with HA overproduction and CD44 is not only functional in MSC but it is expressed in most leukocyte populations. Therefore, CD44 may also provide a mechanism for leukocyte recruitment to sites of injury with potentially detrimental consequences.[29] This is consistent with the finding that CD44$^{-/-}$ mice are protected from ischemic renal injury[29] and, as observed herein, from glycerol-induced ARF. The reduced severity of ARF possibly depends on the inhibition of the recruitment of inflammatory cells. The results of this study indicate that therapeutic administration of exogenous MSC takes advantage of the same molecular mechanism involved in the accumulation of the inflammatory cells within the kidney for their localization at the site of tissue injury. However, it is unclear whether endogenous MSC exploit CD44/HA interaction in the localization at the site of injury.

Taken together, our observations have uncovered an essential role of CD44-mediated HA binding in the recruitment to injured renal tissue of injected exogenous MSC leading to an enhanced renal regeneration.

MATERIALS AND METHODS

Mice

Adult CD44 knockout mice (CD44$^{-/-}$) on C57BL/6 background (Cd44tm1Hbg/J),[51] and adult F2 Hybrid mice (C57BL/6J, 129S1/SvImJ) were purchased from Jackson Laboratory (Bar Harbor, MI, USA). Studies were conducted in accordance with the National Institute of Health Guide for the Care and Use of Laboratory Animals.

Isolation and culture of MSC

CD44^{+}-MSC and CD44$^{-/-}$-MSC from femurs and tibias of 8-week-old mice were obtained as described previously.[52] Cells had a typical spindle-shaped appearance, and the MSC phenotype was confirmed by expression of MSC markers and by ability to differentiate into osteocytes and adipocytes, as described.[1]

Cell migration assay

Twenty-four transwell units were used for monitoring *in vitro* cell migration using 8-μm pore polycarbonate filters (CoStar Corp., Cambridge, MA, USA) as described previously.[53] CD44^{+}-MSC (5×10^{4} cells/well in α-minimum essential medium (α-MEM)), untreated or treated previously for 30 min at 37°C with the blocking rat anti-mouse CD44 mAb (5 μg/ml, clone KM114) (Becton Dickinson, San Jose, CA, USA)[54] were placed in the upper chamber of the transwell unit. α-MEM with 200 or 100 μg/ml HA (from Rooster comb; Sigma, St Louis, MO, USA) was placed in the lower chamber of the transwell unit. CD44^{+}-MSC were allowed to migrate for 18 h through the membrane pores. In selected experiments, different combinations of HA (20 and 200 μg/ml) were added above and below the transwell membrane.

CD44$^{-/-}$-MSC transient transfection

Transient MSC transfectants were generated by electroporation at 250 V and 900 μF in 4 mm electroporation cuvettes in a BIO-Rad

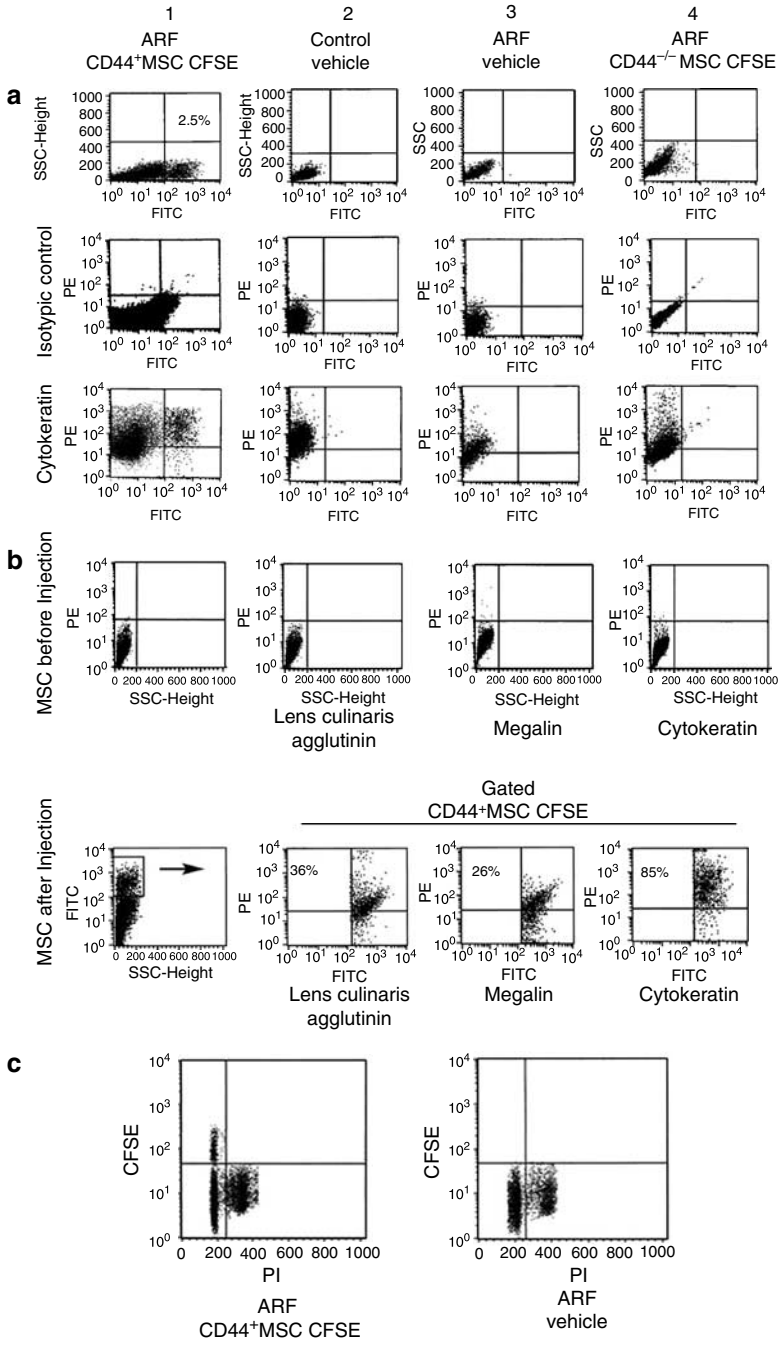

Figure 10 | FACS analysis of CFSE-labelled MSC recovered from renal tissue of ARF mice. (**a**) Column 1: representative flow cytometric analysis of renal cells derived at day 8 from ARF mouse injected with CFSE-labelled CD44$^+$-MSC showing the presence of a population (2.5%) of fluorescent CFSE-positive cells (FITC). Cytokeratin staining (PE) showed that almost all of the CFSE-positive cells were also cytokeratin positive. Column 2 and Column 3: representative flow cytometric analysis of renal cells derived from control mouse without (Column 2) or with ARF (Column 3) injected with vehicle alone, showing no auto-fluorescent cell population. Cytokeratin (PE) was more expressed in cells from healthy mice than in ARF mice, owing to cell damage; no double positive (PE and FITC) cells were detectable. Column 4: representative flow cytometric analysis of renal cells derived from ARF mouse injected with CFSE-labelled CD44$^{-/-}$-MSC showing that only very few fluorescent cells were detectable. Cytokeratin staining (PE) showed that in mice injected with CFSE-labelled CD44$^{-/-}$-MSC only few double-positive cells were detectable. The isotypic controls show the absence of PE auto-fluorescent cells. Five experiments were performed. (**b**): representative flow cytometric analysis of the expression of epithelial markers by CD44$^+$-MSC before and after the injection in ARF mice. In basal condition, MSC did not express the epithelial tubular markers lens culinaris agglutinin, megalin, and cytokeratin. Eight days after ARF the CFSE-positive cells (gate) showed co-staining with the epithelial tubular markers lens culinaris agglutinin, megalin, and cytokeratin, indicating that at least a fraction of CFSE-positive cells expressed epithelial differentiation markers. Five experiments were performed. (**c**) DNA analysis of cells derived at day 8 from ARF mouse injected with CFSE-labelled CD44$^+$-MSC or vehicle. CFSE-positive cells present in ARF mice treated with MSC showed a 2N DNA content. Three experiments were performed with similar results.

Gene-Pulser II Electroporation System (Bio-Rad, Hercules, CA, USA) with 30 μg of the pCDM8 plasmid vector containing full-length CD44H cDNA or CD44R41A mutant of CD44H (CD44HMut) that cannot bind HA.[28] Cells were then plated and used for experiments 72 h after transfection. Transfection efficiency was similar for both constructs ranging between 25 and 30% positive cells by immunofluorescence.

Murine model of ARF and MSC transplantation

To evaluate the ability of $CD44^+$-MSC, $CD44^{-/-}$-MSC and transfected $CD44^{-/-}$-MSC to localize into injured kidney, we induced ARF by i.m. injection of glycerol (Sigma) 7.5 ml/kg[8] and, 3 days after glycerol injection, MSC were intravenously (i.v.) injected into the tail vein. $CD44^+$-MSC, pre-incubated with either an anti-CD44 blocking mAb (KM114, 5 μg/ml) or soluble HA (200 μg/ml) before injection, $CD44^{-/-}$-MSC and transfected $CD44^{-/-}$-MSC (passage III–IV) were harvested using non-enzymatic cell dissociation solution (Sigma). MSC were labelled with 10 μM of CFSE that reacts with the intracellular ammines forming fluorescent conjugates (Vybrant cell tracer kit, Molecular Probes, Eugene, OR, USA) by incubation in α-MEM for 30 min as described previously.[41] In selected experiments, MSC were labelled for 24 h with carboxy-dextran-coated iron oxide nanoparticles (Resovist, Schering, Berlin, Germany).[30] MSC were counted, resuspended in α-MEM (1×10^6 in 150 μl α-MEM) and i.v. injected in glycerol-treated and untreated animals. Mice were killed 24 h or 5 days after transplantation. Localization of iron-labelled MSC was studied only at 24 h because in preliminary experiments, we found that after 3 days iron is dismissed form MSC and can be captured by tubular cells. As control, female mice were injected i.v. with saline 3 days after the glycerol injection. Injected cells were identified using immunohistochemistry with an anti-CFSE polyclonal Ab (pAb), FISH (see below), or Prussian blue to identify iron-loaded cells.[30]

Immunofluorescence, FITC-labelled HA-binding assay and immunohistochemistry

Cytofluorimetric analysis was performed as described.[8]. The following Abs were used: anti-CD105, -CD29, -CD73, -CD34, -CD45, -CD14, -Thy1 mAbs (Becton Dickinson); anti-CD44 mAb (clone KM114); anti-cytokeratin mAb (Biomeda, Foster City, CA, USA), anti-KDR mAb (Chemicon, Temecula, CA, USA), anti-megalin pAb (Santa Cruz Biotechnology, Santa Cruz, CA, USA), lens culinaris agglutinin (Vector Laboratories Inc., Burlingame, CA, USA); phycoerythrin (PE)-conjugated goat against rat immunoglobulin G (IgG) (Sigma) pAb, PE-goat against mouse IgG and against rabbit IgG (DakoCytomation, Copenhagen, Denmark), and PE-rabbit against goat IgG (Santa Cruz) pAbs. The analysis was performed using a FACSCalibur cytometer (Becton Dickinson). A minimum of 10 000 cells were collected for all analyses. CFSE-labelled MSC were detected by FACS analysis after dissociation of the tubular fraction deprived of glomeruli as described previously.[11] For binding studies, cells were incubated with FITC-labelled HA or FITC-labelled bovine serum albumin at 5 μg/10^6 cells, as described.[55] For HA detection, kidney sections were incubated with soluble CD44H-human Ig fusion protein (0.5 μg/ml) prepared as described[19] or human IgG1 isotypic control Ab for 2 h, washed in phosphate-buffered saline and incubated with the FITC-conjugated goat antihuman IgG pAb (Sigma) (1:1000) at 22°C for 30 min.[56] Immunofluorescence on transfected cultured MSC was performed using the antihuman CD44 (clone A3D8) mAb (Sigma). Ethidium bromide (Sigma) was used for nuclear counterstaining. Immunohistochemistry for MSC labelled with CFSE (Molecular Probes) in injured kidney was conducted using an anti-fluorescein/Oregon green pAb (Molecular Probes), as described.[41] The number of CFSE-positive MSC was counted in 10 non-sequential sections for each experiment at magnification $\times$200 and expressed as % in respect to the total number of counted nuclei.

DNA content of engrafted cells

The analysis of DNA content of kidney-migrated CFSE-labelled MSC was performed as described.[57] Briefly, isolated cells were washed in phosphate-buffered saline before 15 min fixation in 4% paraformaldehyde, followed by a fixation in cold acetone for other 15 min. Thereafter, cells were washed in phosphate-buffered saline/bovine serum albumin and were incubated for 2 h at 4°C with propidium iodate (50 μg/ml) (Sigma) to stain the DNA in a solution containing RNAse (200 μg/ml) (Sigma) and 0,1% Tween 20. Cells samples were analyzed on a FACScan (Becton Dickinson).

Fluorescence *in situ* hybridization

Paraffin kidney sections were hybridized with a Starfish Cy3-labeled mouse Y chromosome paint (Star-FISH; Cambio, Cambridge, UK) as previously described.[42] After denaturation at 60°C, slides were incubated with the denatured probe at 37°C overnight, and posthybridization was performed at 37°C by three rinses with 50% formamide/$\times$2 SSC and then $\times$0.1 SSC followed by phosphate-buffered saline. Nuclei were counterstained with Hoechst 33258 dye (Sigma). Images were taken with a Confocal microscope (Carl Zeiss International, Germany).

Morphological studies

Transmission electron microscopy was performed on Karnovsky's-fixed, osmium tetraoxide-postfixed tissues and embedded in epoxy resin according to standard procedures.[58] Ultra-thin sections were stained with uranyl acetate and lead citrate and were examined with a Jeol JEM 1010 electron microscope.

BUN

Blood samples from different groups were collected. Renal function was assessed as BUN in heparinized blood using a on a Beckman Synchrotron CX9 automated chemistry analyzer (Beckman Instruments Inc., Fullerton, CA, USA).

Statistical Analysis

Statistical analysis was performed by using the analysis of variance (ANOVA) with Newmann–Keuls'multicomparison test. A *P*-value of <0.05 was considered significant.

ACKNOWLEDGMENTS

This work was supported by the Associazione Italiana per la Ricerca sul Cancro (AIRC), by Italian Ministry of University and Research (MIUR) FIRB project (RBNE01HRS5-001) and COFIN, by Italian Ministry of Health (Ricerca Finalizzata 02), and by Progetto S Paolo and by MIUR ex60% to BB, LB, and GC.

REFERENCES

1. Pittenger MF, Mackay AM, Beck SC *et al.* Multilineage potential of adult human mesenchymal stem cells. *Science* 1999; **284**: 143–147.
2. Crevensten G, Walsh AJ, Ananthakrishnan D *et al.* Intervertebral disc cell therapy for regeneration: mesenchymal stem cell implantation in rat intervertebral discs. *Ann Biomed Eng* 2004; **32**: 430–434.

3. Chamberlain JR, Schwarze U, Wang PR *et al.* Gene targeting in stem cells from individuals with osteogenesis imperfecta. *Science* 2004; **303**: 1198–1201.
4. Grinnemo KH, Mansson A, Dellgren G *et al.* Xenoreactivity and engraftment of human mesenchymal stem cells transplanted into infarcted rat myocardium. *J Thorac Cardiovasc Surg* 2004; **127**: 1293–1300.
5. Sugaya K. Potential use of stem cells in neuroreplacement therapies for neurodegenerative diseases. *Int Rev Cytol* 2003; **228**: 1–30.
6. Chapel A, Bertho JM, Bensidhoum M *et al.* Mesenchymal stem cells home to injured tissues when co-infused with hematopoietic cells to treat a radiation-induced multi-organ failure syndrome. *J Gene Med* 2003; **5**: 1028–1038.
7. Ortiz LA, Gambelli F, McBride C *et al.* Mesenchymal stem cell engraftment in lung is enhanced in response to bleomycin exposure and ameliorates its fibrotic effects. *Proc Natl Acad Sci USA* 2003; **100**: 8407–8411.
8. Herrera MB, Bussolati B, Bruno S *et al.* Mesenchymal stem cells contribute to the renal repair of acute tubular epithelial injury. *Int J Mol Med* 2004; **14**: 1035–1041.
9. Morigi M, Imberti B, Zoja C *et al.* Mesenchymal stem cells are renotropic, helping to repair the kidney and improve function in acute renal failure. *J Am Soc Nephrol* 2004; **15**: 1794–1804.
10. Thadhani R, Pascual M, Bonventre JV *et al.* Acute renal failure. *N Engl J Med* 1996; **334**: 1448–1460.
11. Bussolati B, Bruno S, Grange C *et al.* Isolation of renal progenitor cells from adult human kidney. *Am J Pathol* 2005; **166**: 545–555.
12. Gupta S, Verfaillie C, Chmielewski D *et al* A role for extrarenal cells in the regeneration following acute renal failure. *Kidney Int* 2002; **62**: 1285–1290.
13. Poulsom R, Alison MR, Cook T *et al.* Bone marrow stem cells contribute to healing of the kidney. *J Am Soc Nephrol* 2003; **14**: S48–54.
14. Hallgren R, Gerdin B, Tufveson G *et al.* Hyaluronic acid accumulation and redistribution in rejecting rat kidney graft. Relationship to the transplantation edema. *J Exp Med* 1990; **171**: 2063–2076.
15. Minguell JJ, Tavassoli M. Proteoglycan synthesis by hematopoietic progenitor cells. *Blood* 1989; **73**: 1821–1827.
16. Wight TN, Kinsella MG, Keating A *et al.* Proteoglycans in human long-term bone marrow cultures: biochemical and ultrastructural analyses. *Blood* 1986; **67**: 1333–1343.
17. Fraser JR, Laurent TC, Laurent UB *et al.* Hyaluronan: its nature, distribution, functions and turnover. *J Intern Med* 1997; **242**: 27–33.
18. Toole BP, Wight TN, Tammi MI. Hyaluronan-cell interactions in cancer and vascular disease. *J Biol Chem* 2002; **277**: 4593–4596.
19. Aruffo A, Stamenkovic I, Melnick M *et al.* CD44 is the principal cell surface receptor for hyaluronate. *Cell* 1990; **61**: 1303–1313.
20. Naor D, Nedvetzki S, Golan I *et al.* CD44 in cancer. *Crit Rev Clin Lab Sci* 2002; **39**: 527–579.
21. Stamenkovic I, Aruffo A, Amiot M *et al.* The hematopoietic and epithelial forms of CD44 are distinct polypeptides with different adhesion potentials for hyaluronate-bearing cells. *EMBO J* 1991; **10**: 343–348.
22. Conget PA, Minguell JJ. Phenotypical and functional properties of human bone marrow mesenchymal progenitor cells. *J Cell Physiol* 1999; **181**: 67–73.
23. Avigdor A, Goichberg P, Shivtiel S *et al.* CD44 and hyaluronic acid cooperate with SDF-1 in the trafficking of human $CD34^+$ stem/progenitor cells to bone marrow. *Blood* 2004; **103**: 2981–2989.
24. Vermeulen M, Le Pesteur F, Gagnerault MC *et al.* Role of adhesion molecules in the homing and mobilization of murine hematopoietic stem and progenitor cells. *Blood* 1998; **92**: 894–900.
25. Khaldoyanidi S, Denzel A, Zoller M. Requirement for CD44 in proliferation and homing of hematopoietic precursor cells. *J Leukoc Biol* 1996; **60**: 579–592.
26. Girard N, Delpech A, Delpech B. Characterization of hyaluronic acid on tissue sections with hyalurectin. *Histochem Cytochem* 1986; **34**: 539–541.
27. Lakshman M, Subramaniam V, Jothy S. CD44 negatively regulates apoptosis in murine colonic epithelium via the mitochondrial pathway. *Exp Mol Pathol* 2004; **76**: 196–204.
28. Peach RJ, Hollenbaugh D, Stamenkovic I *et al.* Identification of hyaluronic acid binding sites in the extracellular domain of CD44. *J Cell Biol* 1993; **122**: 257–264.
29. Rouschop KMA, Roelofs JJTH, Claessen N *et al.* Protection against renal ischemia reperfusion injury by CD44 disruption. *J Am Soc Nephrol* 2005; **16**: 2034–2043.
30. Lange C, Togel F, Ittrich H *et al.* Administered mesenchymal stem cells enhance recovery from ischemia/reperfusion-induced acute renal failure in rats. *Kidney Int* 2005; **68**: 1613–1617.
31. Cantley LG. Adult stem cells in the repair of the injured renal tubule. *Nat Clin Pract Nephrol* 2005; **1**: 22–32.
32. Ji JF, He BP, Dheen ST *et al.* Interactions of chemokines and chemokine receptors mediate the migration of mesenchymal stem cells to the impaired site in the brain after hypoglossal nerve injury. *Stem Cells* 2004; **22**: 415–427.
33. Wynn RF, Hart CA, Corradi-Perini C *et al.* A small proportion of mesenchymal stem cells strongly expresses functionally active CXCR4 receptor capable of promoting migration to bone marrow. *Blood* 2004; **104**: 2643–2645.
34. DeGrendele HC, Estess P, Siegelman MH. Requirement for CD44 in activated T cell extravasation into an inflammatory site. *Science* 1997; **278**: 672–675.
35. Gadhoum Z, Leibovitch MP, Qi J *et al.* CD44: a new means to inhibit acute myeloid leukemia cell proliferation via P27Kip1. *Blood* 2004; **103**: 1059–1068.
36. Thomas L, Byers HR, Vink J *et al.* CD44H regulates tumor cell migration on hyaluronate-coated substrate. *J Cell Biol* 1992; **118**: 971–977.
37. Zhu H, Mitsuhashi N, Klein A *et al.* The role of the hyaluronan receptor CD44 in MSC migration in the extracellular matrix. *Stem cells* 2006; **24**: 928–935.
38. Sy MS, Guo YJ, Stamenkovic I. Inhibition of tumor growth *in vivo* with a soluble CD44-immunoglobulin fusion protein. *J Exp Med* 1992; **176**: 623–627.
39. Wallach-Dayan SB, Grabovsky V, Moll J *et al.* CD44-dependent lymphoma cell dissemination: a cell surface CD44 variant, rather than standard CD44, supports *in vitro* lymphoma cell rolling on hyaluronic acid substrate and its *in vivo* accumulation in the peripheral lymph nodes. *J Cell Sci* 2001; **114**: 3463–3477.
40. Goransson V, Johnsson C, Jacobson A *et al.* Renal hyaluronan accumulation and hyaluronan synthase expression after ischaemia-reperfusion injury in the rat. *Nephrol Dial Transplant* 2004; **19**: 823–830.
41. Togel F, Hu Z, Weiss K *et al.* Administered mesenchymal stem cells protect against ischemic acute renal failure through differentiation-independent mechanisms. *Am J Physiol Renal Physiol* 2005; **289**: F31–F42.
42. Poulsom R, Forbes SJ, Hodivala-Dilke K *et al.* Bone marrow contributes to renal parenchymal turnover and regeneration. *J Pathol* 2001; **195**: 229–235.
43. Duffield JS, Park KM, Hsiao LL *et al.* Restoration of tubular epithelial cells during repair of thepostischemic kidney occurs independently of bone marrow-derived stem cells. *J Clin Invest* 2005; **115**: 1743–1755.
44. Lin F, Moran A, Igarashi P. Intrarenal cells, not bone marrow-derived cells, are the major source for regeneration in postischemic kidney. *J Clin Invest* 2005; **115**: 1756–1764.
45. Broekema M, Harmsen MC, Koerts JA *et al.* Determinants of tubular bone marrow-derived cell engraftment after renal ischemia/reperfusion in rats. *Kidney Int* 2005; **68**: 2572–2581.
46. Fang TC, Alison MR, Cook HT *et al.* Proliferation of bone marrow-derived cells contributes to regeneration after folic acid-induced acute tubular injury. *J Am Soc Nephrol* 2005; **16**: 1723–1732.
47. Maccario R, Moretta A, Cometa A *et al.* Human mesenchymal stem cells and cyclosporin a exert a synergistic suppressive effect on *in vitro* activation of alloantigen-specific cytotoxic lymphocytes. *Biol Blood Marrow Transplant* 2005; **11**: 1031–1042.
48. Zappia E, Casazza S, Pedemonte E *et al.* Mesenchymal stem cells ameliorate experimental autoimmune encephalomyelitis inducing T-cell anergy. *Blood* 2005; **106**: 1755–1761.
49. Prodromidi EI, Poulsom R, Jeffery R *et al.* Bone marrow derived-cells contribute to podocyte regeneration and amelioration of renal disease in a mouse model of Alport syndrome. *Stem Cells* 2006; **24**: 2448–2455.
50. Sugimoto H, Mundel TM, Sund M *et al.* Bone-marrow-derived stem cells repair basement membrane collagen defects and reverse genetic kidney disease. *Proc Natl Acad Sci USA* 2006; **103**: 7321–7326.
51. Protin U, Schweighoffer T, Jochum W *et al.* CD44-deficient mice develop normally with changes in subpopulations and recirculation of lymphocyte subsets. *J Immunol* 1999; **163**: 4917–4923.
52. Jones EA, Kinsey SE, English A *et al.* Isolation and characterization of bone marrow multipotential mesenchymal progenitor cells. *Arthritis Rheum* 2002; **46**: 3349–3360.
53. Bourguignon LY, Zhu H, Shao L *et al.* CD44 interaction with tiam1 promotes Rac1 signaling and hyaluronic acid-mediated breast tumor cell migration. *J Biol Chem* 2000; **275**: 1829–1838.
54. Katoh S, Zheng Z, Oritani K *et al.* Glycosylation of CD44 negatively regulates its recognition of hyaluronan. *J Exp Med* 1995; **182**: 419–429.

55. Nishikawa K, Andres G, Bhan AK *et al.* Hyaluronate is a component of crescents in rat autoimmune glomerulonephritis. *Lab Invest* 1993; **68**: 146–153.
56. Liao H, Lee DV, Levesque MC *et al.* N-terminal and central regions of human CD44 extracellular domain participate in cell surface hyaluronan binding. *J Immunol* 1995; **155**: 3938–3945.
57. Bruno S, Gunetti M, Gammaitoni L *et al. In vitro* and *in vivo* megakaryocyte differentiation of fresh and *ex vivo* expanded cord blood cell: rapid and transient megakaryocyte reconstitution. *Haematologica* 2003; **88**: 379–387.
58. Camussi G, Kerjaschki D, Gonda M *et al.* Expression and modulation of surface antigens in cultured rat glomerular visceral epithelial cells. *J Histochem Cytochem* 1989; **37**: 1675–1687.